Structure and properties of the kagome compound $YBaCo_3AlO_7$

M. Valldor, N. Hollmann, J. Hemberger, and J. A. Mydosh
Institute of Physics II, University of Cologne, Cologne 50937, Germany
(Received 9 May 2008; published 11 July 2008)

Large single crystals of $YBaCo_3AlO_7$ were synthesized in a floating-zone furnace. Powder and single-crystal x-ray data confirm that the structure belongs to the *swedenborgite* compound family ($P6_3mc$, $a=6.28098(3)$ Å, and $c=10.21200(5)$ Å). $YBaCo_3AlO_7$ can reversibly absorb/desorb oxygen up to about $O_{7.5}$ according to thermo gravimetric measurements. The magnetic substructure of corner-sharing $(Co/Al)O_4$ tetrahedra forms kagome-like layers, resulting in a geometric frustration. The magnetization data indicate a highly degenerate spin state with a freezing temperature of $T_f=16.8$ K. Relaxation of magnetic remanence, including aging effects, frequency dependence of ac susceptibility near the transition temperature, and lack of entropy change at T_f allow the conclusion that $YBaCo_3AlO_7$ is a spin glass or a "cluster glass" with randomly frozen domains of antiferromagnetically interacting spins at low temperatures. The origin of this glassy spin state is a combination of Co and Al disorder at the tetrahedral sites and the high frustration between the sites caused by kagome geometry.

DOI: 10.1103/PhysRevB.78.024408 PACS number(s): 75.50.Lk, 75.30.Gw, 75.40.−s

I. INTRODUCTION

Recently, a type of mixed valence metal oxide compound with magnetic kagome substructure was synthesized, $YBaCo_4O_7$. Kagome structures contain strong geometrical frustration, which is a source for exotic magnetic states of antiferromagnetically coupled spins generating spin liquids. As expected, a high degree of magnetic frustration was also indicated by the relatively high Curie-Weiss temperature (−900 K) relative to the spin-freezing temperature ($T_f=65$ K) (Ref. 1). Although there are possibilities for magnetic coupling between the kagome layers, no three-dimensional long-range ordering was indicated in the initial study of $YBaCo_4O_7$.

Similarly to many other complex Co-based oxides, oxygen nonstoichiometry appeared to be yet another degree of freedom, and the compound was reported to absorb up to $O_{8.5}$ per formula unit under pressure,[2] which is the highest relative amount of surplus oxygen in all cobalt oxides per unit weight. The first reported symmetry of the O_7 compound was hexagonal ($P6_3mc$) (Ref. 1), however, extra oxygen causes a reduction in symmetry.[3] The extra oxygen together with reduced symmetry resulted in a putative long-ranged magnetic order, indicated by the Bragg reflections in neutron-diffraction data at low temperatures.[4,5]

Using the chemical doping on the Y site, a magnetic decoupling of the kagome layers was successfully realized in $Y_{0.5}Ca_{0.5}BaCo_4O_7$, which showed only diffuse magnetic scattering from two-dimensional (2D) frustrated magnetic interactions down to 1.5 K (Ref. 6). However, the magnetic decoupling mechanism of the kagome layers could not be fully understood. The question remained, whether high geometrical frustration or an unusual low spin state of tetrahedrally coordinated $Co^{3+}(S=0)$ was the reason for the lack of magnetic coupling between the planes.

Up to now, it has not been possible to synthesize large single crystals of the stoichiometric $YBaCo_4O_7$ or any of its structural homologs, which would help in understanding the material and physical properties. By introducing Al, it was possible to form a congruent melt from which large single crystals could be grown with the composition $YBaCo_3AlO_7$. The previously reported compounds have complex metal valences but this composition contains only $Co^{2+}(S=3/2)$, simplifying the interpretations of magnetic data. Yet other reasons for choosing Al^{3+} were its nonmagnetic nature and its relatively small size; Al could enter the site between the kagome layers, thereby cutting the magnetic interactions between the kagome layers.

II. EXPERIMENT

Large single crystals were synthesized in a floating-zone mirror-image furnace (under flowing Ar, 0.2 dm^3/min). Both feeding bar and seed were prereacted in a corundum boats in air at 1100 °C (20 h) and consisted initially of $BaCO_3$ (Strem Chem. 99.9%), Y_2O_3 (Alfa Aesar 99.99%), Co_3O_4 (Alfa Aesar 99%), and Al_2O_3 (Alfa Aesar 99.95%) in stoichiometric amounts. All polycrystalline bars and the resulting single crystals were opaque and black.

To avoid problems with the high background intensity in the powder-diffraction data due to Co, Cr $Ka_{1,2}$ x-rays ($\lambda=2.28973$ and 2.29365 Å) were used instead of Cu *Ka* as sources in the reflection collection mode (Bragg-Brentano) and a position sensitive detector (PSD) setup (STOE).

Single-crystal data was collected using a STOE IPDS1 working with Mo *Ka* radiation ($\lambda=0.71073$ Å). The crystal was placed in a thin-walled quartz ampoule, avoiding the use of glue. An empirical absorption correction was applied to the obtained diffraction data using STOE software (X-RED and X-SHAPE) (Refs. 7 and 8). During the refinement with the JANA2000 software,[9] all the parameters not restricted by symmetry were refined. Furthermore, the occupancy between the two Co/Al sites (2*a* and 6*c*) was refined, however, constraining the stoichiometry to be ideal ($YBaCo_3AlO_7$). All positions were assumed to be fully occupied.

Gravimetric data was obtained using a thermogravimetric analysis and simultaneous difference thermal analysis (TGA/SDTA) 851^e (Mettler-Toledo), and the data was evaluated

TABLE I. Results from single-crystal refinements of $YBaCo_3AlO_7$. One standard deviation (STD) is presented within parentheses. For the positions 2*a* and 2*b*, the U_{13} and U_{23} parameters have been left out since they are constrained by symmetry.

Wyck.	2*b*	2*b*	2*a*	6*c*	6*c*	2*a*	6*c*
Atom Occ.	Y 1.0	Ba 1.0	Co1 0.56(4) Al1 0.44(4)	Co2 0.81(2) Al2 0.19(2)	O1 1.0	O2 1.0	O3 1.0
x y z	$\frac{2}{3}$	$\frac{2}{3}$	0	0.1707(3)	0.500(5)	0	0.162(3)
	$\frac{1}{3}$	$\frac{1}{3}$	0	0.8293(3)	0.500(5)	0	0.838(3)
	0.8747(4)	$\frac{1}{2}$	0.436(1)	0.6852(8)	0.751(4)	0.249(5)	0.494(3)
Uiso	0.014(2)	0.0120(9)	0.007(2)	0.010(1)	0.05(1)	0.03(1)	0.03(1)
U11	0.014(2)	0.013(1)	0.010(3)	0.012(2)	0.02(1)	0.04(2)	0.06(2)
U22	0.014(2)	0.013(1)	0.010(3)	0.012(2)	0.02(1)	0.04(2)	0.06(2)
U33	0.013(3)	0.010(1)	0.003(3)	0.009(2)	0.09(2)	0.02(2)	0.01(1)
U12	0.007(1)	0.0066(6)	0.005(1)	0.008(2)	0.01(1)	0.017(8)	0.04(2)
U13				0.003(2)	−0.026(8)		0.006(6)
U23				−0.003(2)	0.026(8)		−0.006(6)

Space group: $P6_3mc$, $a=6.28098(3)$ Å, $c=10.21200(5)$ Å, $Z=2$, $\rho_{calc}=5.1577$ g/cm^3, $R_{obs}=0.0716$, R_w(all)$=0.1048$, S(all)$=2.06$, Data/param.$=265/31$, Rest. int. peak/hole$=1.54/-1.71$ e/Å^3

with the standard STAR^e software. The temperature-heating rate was 1 °C/min. Elemental analysis was performed in a scanning electron microscope (SEM515) Philips equipped with an energy dispersive x-ray analysis (EDAX) unit at 20 kV acceleration voltage.

Magnetic investigations were done with a physical property measurement system (PPMS) Quantum Design, equipped with a vibrating-sample magnetometer (VSM) device in a field of up to 1 T in the temperature range 3–400 K. This PPMS was also used for performing the specific-heat measurements without magnetic fields. AC magnetization was realized in a superconducting quantum interference device (SQUID) magnetic property measurement system (MPMS) XL Quantum Design, with driving frequencies between 1 and 23 Hz, and an amplitude of 2.5 Oe.

III. RESULTS

A. Composition

The single crystal was cut into slices, one of which was polished to high reflectivity, and the surface was examined in a microscope using polarized light. The whole sample contained only one crystal domain as the surface had equal reflectivity when changing the polarization. In the electron microscope, 10 energy dispersive x-ray (EDX) analyses on different spots on the surface gave the metal composition $Y_{0.8(1)}Ba_{1.05(4)}Co_{3.2(1)}Al_{0.95(5)}$, assuming all metals to add up to 6. This is close to the desired stoichiometry, and the deviations are probably due to the standards in the EDX software, e.g., Y metal is used as standard instead of Y_2O_3.

From the x-ray absorption spectroscopy (XAS) data close to the Co-*L* edge and O-*K* edge, it was possible to conclude that Co is mainly divalent.[10] The amount of Co^{3+} was estimated to be below 3%, meaning the maximum oxygen content per unit formula would be $O_{7.06}$.

B. X-ray diffraction

Using powder-diffraction data from a well-ground single crystal, the unit-cell parameters for the hexagonal unit cell ($P6_3mc$) were refined to $a=6.28098(3)$ and $c=10.21200(5)$ Å. In comparison, the cell parameters from the single-crystal investigation were both larger ($a=6.287(1)$, $c=10.231(3)$ Å) due to a small error in the crystal to image plate distance. Thus, the more accurate *a* and *c* from the powder data are presented in the single-crystal data (Table I). By keeping the 2*a* metal position fully occupied by Al and the corresponding 6*c* site with only Co, the refinement of the single-crystal data resulted in the negative thermal displacement of the 2*a* site. Hence, Al/Co mixing between the 2*a* and 6*c* was necessary to obtain reasonable *U* values. The structure agrees well with the observed diffraction intensities, giving a reasonable figure of merit ($S=2.06$), and low rest-electron densities (± 1.6 e$^-$/Å^3). Hence, according to single-crystal electronic densities, it was not possible to fully decouple the magnetic kagome layers by the nonmagnetic Al.

A detailed description of the structure (Fig. 1) can be found elsewhere.[1] However, to aid the discussion below, a brief description follows here. Three types of oxygen coordinations are present: an anticuboctahedron (CN=12) for Ba, an octahedron (CN=6) for Y, and tetrahedra (CN=4) for Co and Al. The tetrahedra form a wurzite-like substructure, where Ba replaces four tetrahedra; this results in Co/Al containing kagome layers perpendicular to *c*, described by one crystallographic site (6*c*). Connecting the layers along *c* is the second Co/Al (2*a*) site. The superexchange angles via oxygen along *c* are Co1-O2-Co2$=109(1)°$ and Co1-O3-Co2$=111(1)°$, and the in-kagome-plane exchange angles are Co2-O2-Co2$=110(1)°$ and Co2-O1-Co2$=106(2)°$. The metal to oxygen distances are presented in Table II, together with the corresponding bond valence sums (BVSs). Most of the calculated values are significantly different from the expectation values, which should mean that the system contains relatively high covalency; summing up the metal valences, according to BVS gives $\approx +13$, one charge lower than expected. It is unlikely that the structure would lack oxygen because this would mean that the very

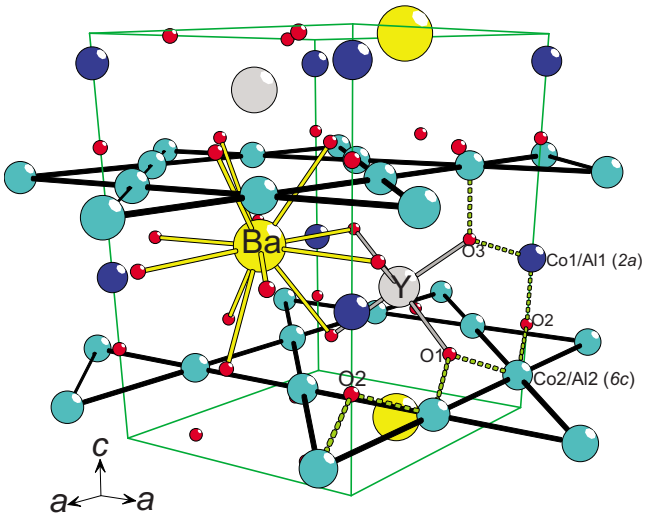

FIG. 1. (Color online) A perspective view of the atomic structure of $YBaCo_3AlO_7$. The smaller balls (red) are oxygen atoms, and the three different sites are marked with O1, O2, and O3. The oxygen coordination of Y and Ba are indicated with bonding lines between the metals and oxygen atoms. The kagome net is highlighted with thick lines between the Co2 (light blue) sites. The Co1 (blue) sites connect the layers. The hexagonal unit cell is marked with a thin green line, the coordination system is shown, and dashed green lines indicate the different (Co/Al)-O-(Co/Al) angles discussed in the text.

unstable trigonal-planar-coordinated Co^{2+} has to be present. It is easier to accept the covalent situation where oxygen is in average −1.86.

C. Oxygen storage capacity

Since the $YBaCo_4O_7$ was reported to absorb and desorb reproducibly an unusually large amount of oxygen at elevated temperatures,[2] thermogravimetry was also carried out on the Al containing sample presented here. In nitrogen atmosphere, there is no weight gain (not shown) but the sample readily oxidizes in oxygen atmosphere [Fig. 2(a)]. The temperature-dependent oxygen stoichiometry changes similarly to that of $YBaCo_4O_7$, however, the amplitude is significantly smaller: $YBaCo_3AlO_{7.25}$ is found at 305 °C at 1 bar of O_2. The reversibility of the oxygen absorption/desorption shown in Fig. 2(b) was tried in the same way done by Karppinen *et al.*[2] at a constant temperature close to the maximum in Fig. 2(a). The oxygen uptake seems reversible but the amount increases (diverges) in the second cycle. This could mean that the main reaction happens at the grain surfaces; the first cycle creates cracks and defects in the grains, and a larger surface area is therefore obtained before the second charging step starts. This, however, needs to be further investigated. The oxygen content per unit formula is at the end of the second cycle at about 7.6. The small jumps in weight as the gas is changed are due to the different densities of O_2 and N_2.

D. Magnetic investigations

$YBaCo_3AlO_7$ exhibits slightly anisotropic magnetic behavior below room temperature (Fig. 3). No single-ion anisotropy would be expected since Co^{2+} in the configuration $e^4t_2^3$ has a full e shell and a half-filled t_2 shell. Thus, the orbital momentum is completely quenched, explaining the isotropic behavior at high temperatures. The anisotropy below room temperature is probably caused by the complex magnetic interaction in and between the kagome layers. Down to 30 K, the susceptibility in the c direction is somewhat higher, but at the spin-glass-like cusp at T_f=16.8 K, the *ab plane* exhibits the higher susceptibility. Below the freezing temperature T_f, the susceptibility is different for zero-field-cooling (ZFC) and field-cooling (FC) measurements, indicating the nonergodicity of the glassy ground state. Note that this behavior is also anisotropic since the *ab plane* shows a larger splitting between ZFC and FC curves.

Huq *et al.*[3] observed a magnetic feature close to 300 K in $YbBaCo_4O_{7+\delta}$, which was interpreted as a structural phase transition. However, this feature is not seen for $YBaCo_3AlO_7$ below 400 K, which might be due to the fact that the present compound is close to oxygen stoichiometric ($\delta \approx 0$).

In Fig. 3(b), the inverse susceptibility is shown. It can be seen from the form of the curve that one should be cautious in using a Curie-Weiss law. At least for high temperatures, the effective moment can be roughly estimated to be 2.8 μ_B per Co ion, which is lower than the value of $Co^{2+}(S=3/2)$ of 3.87 μ_B. In addition, the extrapolated Curie-Weiss constant is very high compared to the freezing temperature: $\theta_{CW}/T_f \approx 28$. These properties evidence the strong degree of frustration present in $YBaCo_3AlO_7$.

The magnetic hysteresis originates from a highly irreversible and metastable state, as magnetic relaxation is seen in the field-cooled state [Fig. 4(a)]. Furthermore, the relaxation rate also depends on the waiting time used by letting the frozen magnetic state solidify: a slower relaxation is realized

TABLE II. Metal to oxygen distances in Å calculated from the single-crystal data and their multiplicity. The last row contains the corresponding BVSs for the different metal sites as described by Brown and Altermatt (Ref. 11).

Oxygen\Metal	*Y*	Ba	(Co/Al)1	(Co/Al)2
O1	3×2.21(4)	6×3.14(4)		2×1.91(3)
O2			1×1.91(5)	1×1.97(2)
O3	3×2.22(2)	6×3.14(2)	3×1.86(2)	1×1.96(3)
BVS	3.53	1.19	2.46(Co), 2.03(Al)	2.07(Co), 1.70(Al)

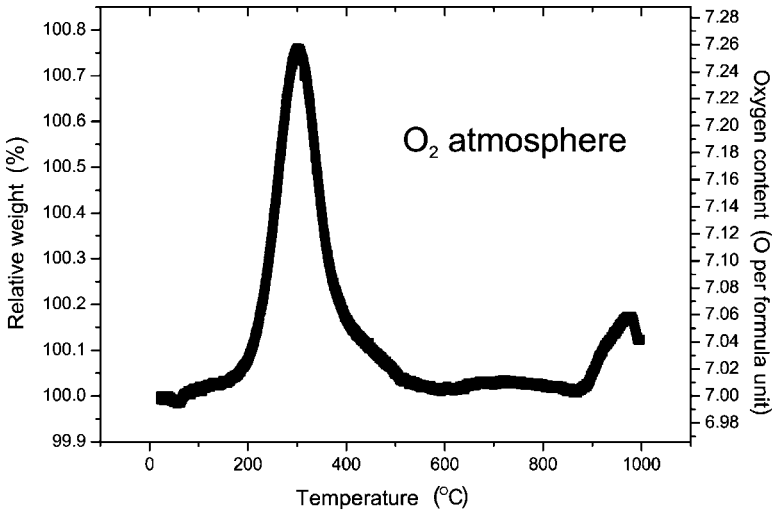

(a)

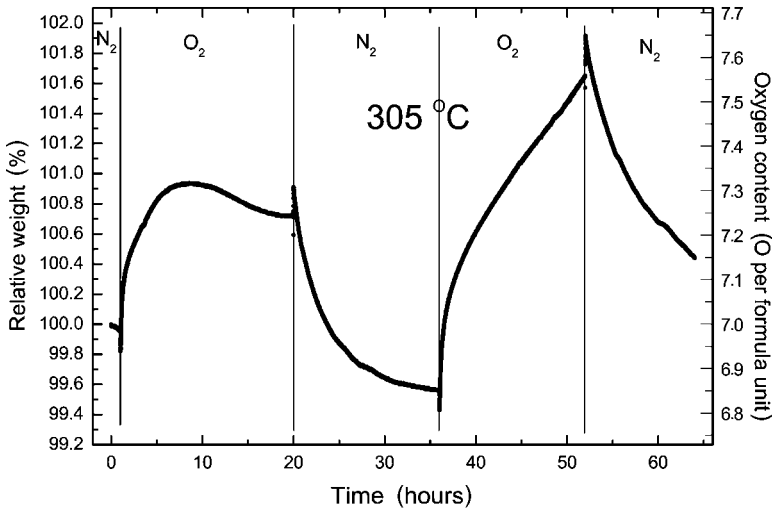

(b)

FIG. 2. Thermogravimetric data of a powdered $YBaCo_3AlO_7$ single crystal. (a) Heat treatment in oxygen atmosphere (50 ml/min). The oxygen content has been calculated with the assumption that the starting compound had the ideal stoichiometry. (b) Weight changes at isothermal conditions (305 °C). The flowing gas (N_2 or O_2) has been changed at the vertical lines. The oxygen content has been calculated as in Fig. 2(a).

by longer waiting time before removing the external field. This property is archetypal for spin-glass-like materials around and below the glass freezing temperature T_f. The observed amount of magnetic remanence, a few percent, is also typical for spin glasses. However, the spin-glass-like state appears to be anisotropic; applying the field along the unique axis (c) resulted in a higher remanence [Fig. 4(b)] with a factor of more than three, although the larger difference between FC and ZFC is seen with the field perpendicular to c [Fig. 3(a)]. The relaxations along the two crystallographic directions follow different initial time dependences and, yet after 1000 s, the relaxation rates are almost identical; the two ordinate scales in Fig. 4(b) have the same interval size to make this clear.

To further probe the dynamic of the spin structure, ac susceptibility at different frequencies was employed with small driving field (2.5 Oe). As can be seen in Fig. 5, the transition temperature exhibits a clear frequency dependence $T_f(\omega)$, i.e., for higher frequencies T_f, as denoted by the maximum in χ', increases. At the same time, the imaginary part of the magnetic susceptibility (χ'') exhibits a step-like increase, which is typical for a spin glass (lower inset in Fig. 5). Also, the onset of absorption (χ'') accompanies T_f and shifts similarly with changing ac frequency. To resolve whether $YBaCo_3AlO_7$ is more a superparamagnet or a well-coupled spin glass, the dynamic exponent (zv) was extracted by plotting the frequency dependence of the relative T_f and fitting a linear function (upper-right inset in Fig. 5): a dynamic exponent of 5.6 and a normalized frequency shift of 0.02 indicate that a spin glass better describes the present spin system.[12]

E. Specific heat

There are no indications for anomalies in specific heat over the whole measured temperature range (2–300 K) due to structural or magnetic phase transitions (Fig. 6). At low temperatures, the normal T^3 proportionality is seen. At higher temperatures, an increase toward saturation is observed due to the phonon maximum. For the low-temperature region ($T \leq 10$ K in Fig. 6), the Debye temperature (θ_D) was estimated to be 85 K. The reason for this low value requires further investigation. The subtle effects of the spin glass freezing around 17 K in the specific heat were not detected because of the large phonon contribution.

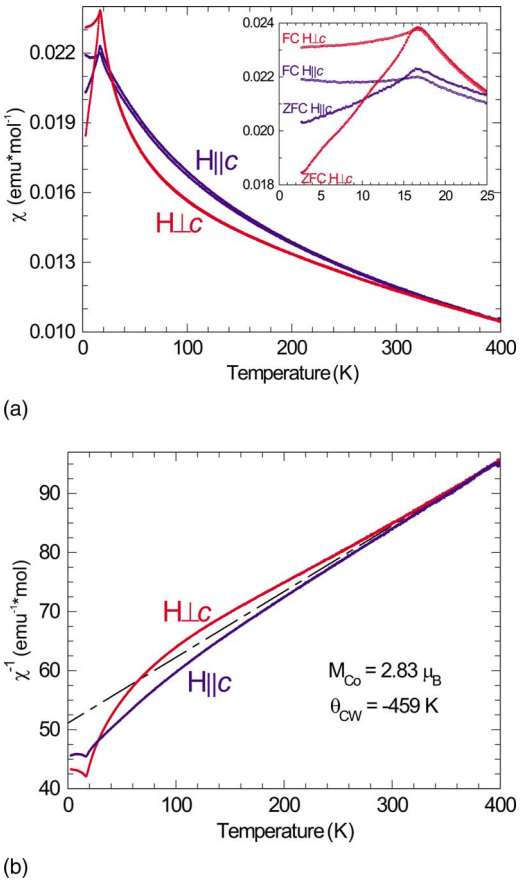

FIG. 3. (Color online) (a) The magnetic-susceptibility (χ) is plotted as function of temperature for $YBaCo_3AlO_7$. The two data sets represent the measurement with the field (H) parallel and perpendicular to the unique axis (c). The inset upper right is a magnification of the low-temperature region. (b) The same data as in Fig. 3(a) is again plotted but χ is displayed on a reciprocal scale. The dashed line represents a Curie-Weiss fit to extract the paramagnetic moment and the Weiss constant (θ_{CW}).

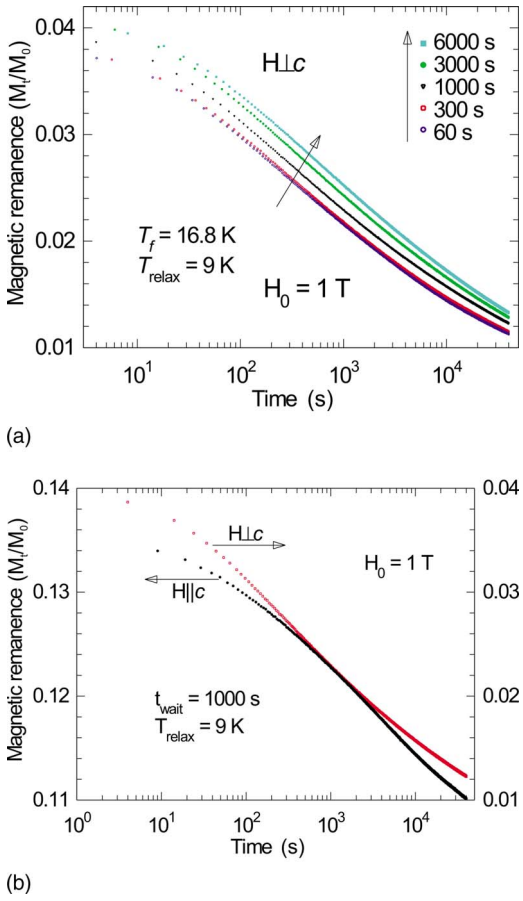

FIG. 4. (Color online) (a) Magnetic relaxation with different waiting times before shutting of the outer field. A field cooling was performed down to 9 K, 7.8 K below the magnetic freezing temperature with a subsequent waiting time (t_{wait}–upper right) to let the disordered state solidify before the outer field was shut off, and the residual magnetic signal defined as magnetization at time $t(M_t)$ divided by the magnetization with field (M_0) was recorded as function of time. The curves represent different t_{wait} as indicated at upper right in the figure. The field was applied perpendicular to the unique axis (c). (b) The anisotropy of the relaxation is shown in for H parallel and perpendicular to c using the same t_{wait}(=1000 s). The scale for the $H \| c$ data is displayed left and for the $H \perp c$ on the right side. In both graphs, only every 10th data point is shown.

IV. DISCUSSION

According to the single-crystal data, we were not successful to use Al to magnetically decouple the kagome layers, however, the random substitution of Al^{3+} at the two crystallographic Co^{2+} sites induces a frustrated magnetic state, e.g., a spin glass. The $YBaCo_3AlO_7$ composition melts congruently, making it possible to grow large single crystals from the melt, such has not yet been achieved for stoichiometric $YBaCo_4O_7$ without the use of a flux.[13]

Within the structure of $YBaCo_3AlO_7$, (i) all Co-O-Co angles are close to the tetrahedral angle (109.5 °), which is not associated with a strong superexchange. Also, (ii) a strong covalent bond character is possible since the BVS calculations fail completely. Combining facts (i) and (ii), the strong magnetic interactions can be understood by introducing orbital hybridization between oxygen and cobalt, i.e., if the oxygen orbitals would be sp^3 hybridized, the tetrahedral angle would result in a strong orbital overlap.

The reason for having different oxygen absorption between $YBaCo_4O_7$ and $YBaCo_3AlO_7$ could be due to the larger presence of Co^{3+} in the former compound. Co^{3+} is known to form more covalent bonding to oxygen, which is also a step toward nondefined oxidations states. The site for the extra oxygen atoms has now been identified by Chmaissem *et al.*[14] resulting in a transformation of tetrahedra into octahedra and a strong structural distortion.

For isostuctural compounds $REBaCo_4O_7$ (RE=Lu, Yb, Tm), spike-shaped peaks were seen in the specific-heat measurements and anomalies occurred in the resistivity between 150 and 200 K, indicating first-order structural phase transitions:[15] the authors interpreted these transitions as changes in symmetry from high-temperature hexagonal to low-temperature orthorhombic. These changes in symmetry were also reported for the systems $YbBaCo_4O_7$ from high-resolution neutron diffraction,[4] and it was suggested that the high-temperature symmetry is trigonal, which transforms

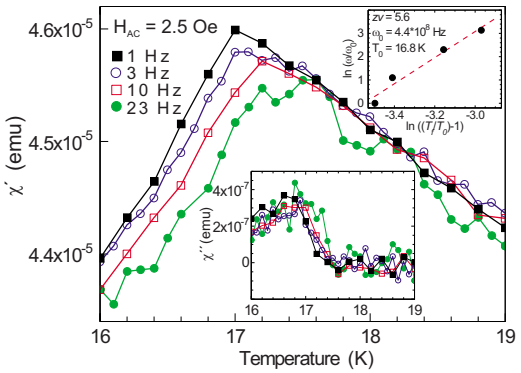

FIG. 5. (Color online) Frequency-dependent ac susceptibility with the field parallel to the 001 axis of $YBaCo_3AlO_7$. The lower inset shows the imaginary part of the susceptibility and the upper-right inset is a power plot, where the frequency is plotted as function of the relative transition temperature. The dashed line represents a linear fit to extract the dynamic exponent ($z\nu$) and the upper frequency limit (ω_0).

into orthorhombic at lower temperatures. Using x-ray diffraction, it was not possible to detect a lower symmetry than hexagonal at room temperature for $YBaCo_3AlO_7$, and there are no indications for a lowering of symmetry below 300 K, i.e., no first-order transition in the specific-heat measurements or in the magnetic-susceptibility curves. Furthermore, no Co^{3+} could be detected in the XAS data.[10] We therefore assume that the compound presented here is very close to being oxygen stoichiometric, which stabilizes the relatively high hexagonal symmetry ($P6_3mc$).

Magnetic and crystallographic data for powder samples of two closely related compounds have previously been published: (i) $CaBaCo_3AlO_7$ (a=6.3065(5), c=10.1205(8) Å) with T_f=22 K, frequency-dependent $\chi'(w)$ and $\chi''(\omega)$, yet almost no relaxation of magnetic hysteresis[16] and (ii) $YBaCo_3ZnO_7$ (a=6.3053(3), c=10.276(1) Å) with T_f =27 K, exhibiting $\chi(\omega)$ and $\chi''(\omega)$ with, indeed, relaxation of the magnetic hysteresis.[17] From the changes in unit cell size between the three different substitutions, it is possible to see that Al in $YBaCo_3AlO_7$ is not fully situated between the

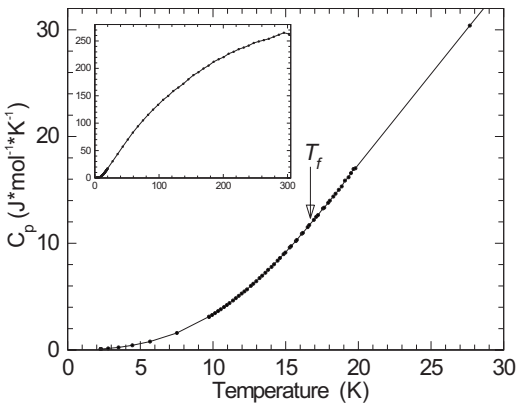

FIG. 6. Low-temperature specific-heat data for $YBaCo_3AlO_7$ measured in zero field. Lines are drawn to guide the eye, and T_f from the magnetic data is indicated. The upper inset shows the data up to room temperature.

layers; the c axis is much shorter in $CaBaCo_3AlO_7$, which here is a clear indication of high Al presence between the layers. Also situated between the kagome layers, Y^{3+} might be the reason for elongating the c axis, thereby forcing Al to become distributed among all tetrahedra in the structure. Independent on the substitution in the tetrahedral net, nonmagnetic Al and Zn probably cause the magnetic properties to become more random, as a frequency-dependent ac magnetic susceptibility (in real and imaginary parts) is seen for both $CaBaCo_3AlO_7$ and $YBaCo_3ZnO_7$. A similar ac-field frequency dependence is seen for $YBaCo_3AlO_7$ and the dynamic exponent ($z\nu$) is close to what is expected for spin glasses. $YBaCo_3ZnO_7$ and $YBaCo_3AlO_7$ show relaxation of magnetic hystereses but $CaBaCo_3AlO_7$ exhibits virtually no relaxation or perhaps, a very short-lived relaxation. Note that the Ca substitution does not lead to magnetic dilution in the same sense as for Zn and Al, both of which enter the magnetic substructure. This could mean that the observed magnetic relaxation is dependent on the presence of interplanar magnetic coupling, which is most likely lacking in $CaBaCo_3AlO_7$.

Interesting is the fact that the magnetic behavior and relaxations for the two different crystallographic direction in $YBaCo_3AlO_7$ are different. To understand this, a few facts have to be gathered. (i) Although no long-range magnetic order is present, there is a tendency for strong 2D interactions in the kagome layers. For comparison, in the closely related $Y_{0.5}Ca_{0.5}BaCo_4O_7$ system,[6] it was shown that a chiral 2D spin state called $\sqrt{3}\times\sqrt{3}$ (Ref. 18) is present. Although these spins are fluctuating, their contribution to the magnetization perpendicular to the plane is relatively small, which would accommodate the anisotropy seen in Fig. 3(a). (ii) The different amounts of magnetic remanence [Fig. 4(b)] for the different crystallographic directions can be caused by magnetic anisotropy, i.e., the magnetic moments along 001 are easier to align.

A plausible model for the spin system in $YBaCo_3AlO_7$ when adding [i] and [ii] is that the kagome layers contain spins that are almost fully oriented within the layers and at the interplanar site, the spin is mainly oriented along 001. Furthermore, the spin-spin interactions are stronger within the kagome layers but weaker at the interlayer site. Note that the random-site disorder in $YBaCo_3AlO_7$ is essential for the spin-glass properties, since the random-bond system $Y_{0.5}Ca_{0.5}BaCo_4O_7$ exhibits very different properties. This necessitates further studies on the random-bond situation to understand the resulting ground state. In conclusion, $YBaCo_3AlO_7$ can be described as an anisotropic random-site spin glass with possible inclusions of antiferromagnetic domains with extremely short coherence lengths.

ACKNOWLEDGMENTS

We acknowledge Ingo Pantenburg at the Inorganic Chemistry Department (Cologne University) for providing us with the single-crystal x-ray data. We thank Susanne Heijligen for performing the thermogravimetric investigations. We are also grateful for the elemental analyses done by Inge Simons. This work was supported by DFG through the project SFB 608.

[1] M. Valldor and M. Andersson, Solid State Sci. **4**, 923 (2002).
[2] M. Karppinen, H. Yamauchi, S. Otani, T. Fujita, T. Motohashi, Y.-H. Huang, M. Valkeapää, and H. Fjellvåg, Chem. Mater. **18**, 490 (2006).
[3] A. Huq, J. F. Mitchell, H. Zheng, L. C. Chapon, P. G. Radaelli, K. S. Knight, and P. W. Stephens, J. Solid State Chem. **179**, 1136 (2006).
[4] L. C. Chapon, P. G. Radaelli, H. Zheng, and J. F. Mitchell, Phys. Rev. B **74**, 172401 (2006).
[5] M. Soda, Y. Yasui, T. Moyoshi, M. Sato, N. Igawa, and K. Kakurai, J. Magn. Magn. Mater. **310**, e441 (2007).
[6] W. Schweika, M. Valldor, and P. Lemmens, Phys. Rev. Lett. **98**, 067201 (2007).
[7] X-RED, STOE & Cie GmbH, Darmstadt, Germany, Version 1.07, 1996.
[8] X-SHAPE, STOE & Cie GmbH, Darmstadt, Germany, Version 1.01, 1996.
[9] V. Petříček and M. Dušek, JANA2000, Institute of Physics AVCR, Praha, Czech Republic, 2002.
[10] N. Hollmann, Z. Hu, and L. H. Tjeng (private communication).
[11] I. D. Brown and D. Altermatt, Acta Crystallogr., Sect. B: Struct. Sci. **41**, 244 (1985).
[12] J. A. Mydosh, *Spin Glasses: An Experimental Introduction* (Taylor & Francis, London, 1993).
[13] L. G. Bychkov, S. V. Shiryaev, A. G. Soldatov, A. S. Shestak, S. N. Barilo, D. V. Sheptyakov, K. Conder, E. Pomjakushina, A. Podlesnyak, A. Furrer, and R. Bruetsch, Cryst. Res. Technol. **40**, 395 (2005).
[14] O. Chmaissem, H. Zheng, A. Huq, P. W. Stephens, and J. F. Mitchell, J. Solid State Chem. **181**, 664 (2008).
[15] N. Nakayama, T. Mizota, Y. Ueda, A. N. Sokolov, and A. N. Vasiliev, J. Magn. Magn. Mater. **300**, 98 (2006).
[16] M. Valldor, J. Phys. Chem. Solids **66**, 1025 (2005).
[17] M. Valldor, J. Phys.: Condens. Matter **16**, 9209 (2004).
[18] J. N. Reimers and A. J. Berlinsky, Phys. Rev. B **48**, 9539 (1993).